

# Strong Internal Tides in the Strait of Gibraltar: Measurements and Modelling

E. G. Morozov<sup>1</sup> <sup>a</sup> and M. G. Velarde<sup>2</sup>

<sup>1</sup>*Shirshov Institute of Oceanology, Russian Academy of Sciences, 36 Nakhimovsky prospekt, Moscow, Russia*

<sup>2</sup>*Instituto Pluridisciplinar, 1 Paseo Juan XXIII, Madrid, Spain*

**Keywords:** Strait of Gibraltar, Internal Waves, Numerical Modeling.

**Abstract:** We analyze moored current measurements in the Strait of Gibraltar. Internal waves are extremely strong in the strait. The vertical displacements of water particles with a semidiurnal frequency sometimes exceed 200 m. These displacements are associated with forced tidal internal waves over the Camarinal Sill, which crosses the strait. The amplitudes of the waves decrease with the distance from the sill, and at a distance of 50 km from the sill, the amplitudes are three times smaller than over the sill. Numerical modelling shows that the lower current in the strait directed from the Mediterranean Sea to the ocean has a significant influence on internal tides. The effect of internal waves propagating in a hydraulic flow leads to the formation of internal bore, followed by a wave packet of shorter internal waves.

## 1 INTRODUCTION

The Strait of Gibraltar (Fig. 1) has been known from the ancient ages. It is characterized by a two-layer system of opposite flows resulting from the difference in water density between the Atlantic Ocean and the Mediterranean Sea. A strong surface current of relatively fresher water from the ocean compensates for intensive evaporation in the Mediterranean. A deep-water current of more saline Mediterranean water flows into the ocean. A barotropic tidal wave is imposed on this system with velocities in the range 70-80 cm/s, about the same order of magnitude as the mean velocities of the currents between the ocean and the sea, and thus, an unsteady flow is formed. The tide generates a strong tidal internal wave, when the tidal currents flow over uneven topography in the strait.

The estimate for the Mediterranean water outflow is equal to  $-0.68 \text{ Sv}$  ( $1 \text{ Sv} = 10^6 \text{ m}^3/\text{s}$ ), while the flow of Atlantic waters is  $0.72 \text{ Sv}$ , which equals to the sum of the outflow and net evaporation that is approximately 52 cm of the sea level per year (Bryden et al., 1994; Morozov et al., 2002, 2003).

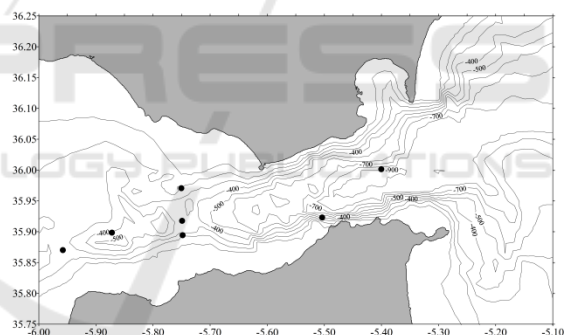



Figure 1: Chart of the Strait of Gibraltar and locations of moorings (black dots).

## 2 MOORED MEASUREMENTS

Moored measurements in the strait reveal very strong internal waves whose double amplitude (vertical displacements of particles) can be as high as 200 m over a depth of 400 m. The displacement of  $13^\circ\text{C}$  isotherm gives the best illustration of such a displacement. The vertical displacement ranges from 100 to 300 m (Fig. 2). To estimate the wavelength of the semidiurnal waves we used the antenna method developed in

<sup>a</sup>  <https://orcid.org/0000-0002-0251-3454>

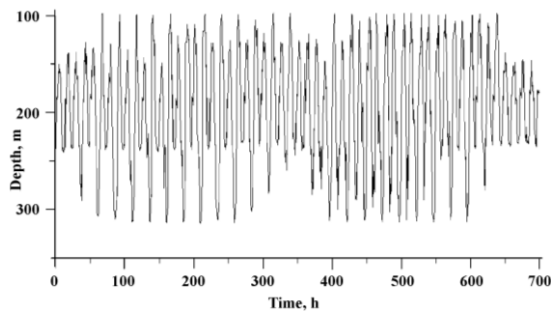


Figure 2: Depth variation of 13°C isotherm from July 2 to July 31, 1986.

seismology and applied for oceanic waves by Barber (1963) assuming arbitrary position of the wave sensors. The method is based on the calculation of the cross spectra for each pair of the possible combinations of sensors with further convolution at the semidiurnal frequency of the waves. The amplitude and phase cross-characteristics of the oscillation are used to calculate the spatiotemporal spectra at the wave frequency and estimate the components of the horizontal wave number. The method basically accounts for the statistical phase difference between each pair of wave sensors.

The wave propagating to the east of the sill was estimated on the basis of 16 different combinations of moorings. The wave propagates to the east in the azimuth interval between 90 and 120 degrees, while the wavelength ranges between 90 and 140 km.

### 3 NUMERICAL MODELING

In order to model the wave propagation we use the fully nonlinear non-hydrostatic model of the baroclinic tides developed by (Vlasenko, 1992; Morozov et al., 2002). We consider a two dimensional ( $x, z$ ) flow in a continuously stratified rotating ocean of variable depth.

Although the model is two dimensional, we introduce the equation for the V-component of velocity normal to the  $x, z$  plane to account for the effects of rotation. However, the V-component is considered constant. For convenience, the equation of density diffusion has been used instead of the equations of heat and salt diffusion.

The boundary conditions at the surface located at  $z = 0$  are zero for the density gradient, vorticity, and stream function; hence, no tangential stresses are considered. We also consider zero vertical motion and no heat and salt transport through the surface.

At the bottom, no heat, salt, and mass transports exist. The boundary condition for vorticity at the bottom is calculated using equation  $\Omega = \Delta\Psi$  with the value of the stream function field  $\Psi$  obtained at the previous time step.

The wave perturbations of vorticity, stream function, and density are assumed zero at the lateral boundaries located far from the bottom irregularities at the submarine ridge. The calculations start from a state of rest when the fluid at the bottom is motionless, and the isopycnals are horizontal; hence: at  $t=0$ :  $\Omega=0$ ,  $\rho=0$ ,  $\Psi=0$ . We stop the calculations, when the wave perturbations reach the lateral boundaries. The phase velocity of the perturbations does not exceed 2-3 m/s, which allows us to continue the calculations for a suitable number of time steps.

The bottom topography was introduced in the model from the digital databases of bottom topography. We specify a density field unperturbed by internal waves corresponding to the vertical distribution of the Brunt-Väisälä frequency  $N(z)$  from observations.

A semi-implicit numerical scheme utilizes a rectangular grid with second order approximations to the spatial derivatives and first order approximation of the temporal derivatives in every temporal semi-layer. At each time step, the implicit system, which is a tri-diagonal matrix, is solved using standard techniques.

We model the following physical phenomenon. A long barotropic tidal wave propagates from the open ocean to the continental slope or submarine ridge. The tidal currents flow over the topographic obstacles and obtain a vertical component. Periodically oscillating vertical components with a tidal period displace water particles; thus a tidal internal wave is generated. The input parameters of the model are stratification, bottom topography, and stream function of the tidal current. The model outputs the fields of density and velocity over the domain of calculations.

We have chosen a domain 300 km long with a horizontal step of 200 m and 20 vertical levels. The horizontal size of the domain significantly exceeds the size of the strait, but allows us to analyze the processes in the middle of the domain before the perturbations reach the lateral boundaries. The time step was approximately equal to 7 seconds. These parameters satisfy the Courant-Friedrichs-Levy condition. The coefficients of the horizontal eddy viscosity and density diffusivity were fixed to 60  $\text{m}^2/\text{s}$  over the ridge and 4  $\text{m}^2/\text{s}$  beyond the ridge over the flat bottom in the model. Strong motion at the

slopes of the sill requires great values of the coefficients. The coefficients of vertical turbulent viscosity and density diffusion were set to  $0.001 \text{ m}^2/\text{s}$ .

The main objective of the model investigation is to study the influence of the currents on internal tide propagation in the Strait. In the first version of model calculations we make the approximation of the model with zero mean current. We introduce only a periodical barotropic tidal flow by periodical increasing and decreasing the value of the stream function at the surface, while the value of the stream function at the bottom is specified equal to zero. The maximum value of the stream function was chosen to provide the maximum horizontal tidal velocities equal to  $80 \text{ cm/s}$ . The period of reciprocating flow is 12.4 hours.

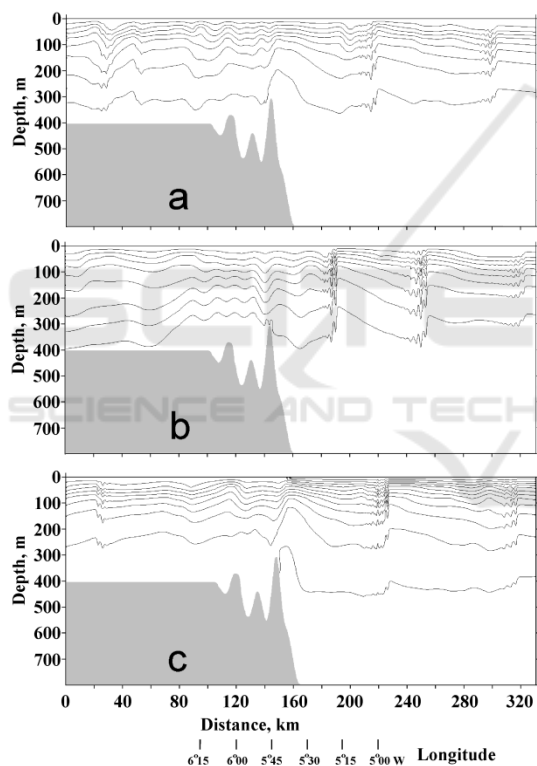


Figure 3: Perturbations of the density field induced by propagating internal tide. The contour lines of density are shown with an interval of  $0.00025 \text{ g/cm}^3$ . Grey coloured pattern shows bottom topography. The density perturbations develop on the background of different currents in the strait:

- (a) Zero mean current
- (b) Westward barotropic current
- (c) Oppositely directed inflowing and outflowing currents.

The periodical changes in the horizontal flow induce an internal wave propagating in both

directions from the sill positioned in the middle of the computation area. The perturbations of the density field induced by propagating internal tide are shown in Fig. 3a. This snapshot of the density field is depicted after four tidal periods of calculation. The fluctuations of the density field are not symmetrical with respect to the position of the Camarinal Sill because the bottom topography is not symmetrical. Camarinal Sill is strongly abrupt at the eastern slope, while the bottom topography is more corrugated and the mean inclination of the slope is smaller west of the sill. A calculation, when the bottom topography was specified only by a symmetric sill, gave a symmetric pattern of propagating fluctuation in both directions from the sill.

Internal bore is formed on the trailing edge of the wave, which is steeper than the leading edge. A packet of shorter internal waves follows the bore. The structure of the westerly propagating wave is the same except for the fact that the bore and wave train of shorter internal waves are less intensive in the western part compared to the eastern part of the basin.

In the second version of model calculation we introduce a steady barotropic westward current in the entire water column of the Strait by specifying the permanent value of the stream function at the surface and zero at the bottom so that the velocity of the mean current is equal to  $30 \text{ cm/s}$  at the western boundary. At the eastern boundary the velocity is equal to  $18 \text{ cm/s}$ . The mean velocity over the sill is equal to  $41 \text{ cm/s}$ . We superimpose a periodical barotropic tidal current on the mean current as done in the previous step. At the western boundary, the maximum amplitude of the barotropic tidal velocity is  $80 \text{ cm/s}$ , the same as it was without the mean current.

The westward flow changes the internal wave field (Fig. 3b). In the eastern part, where the internal tide propagates opposite to the current, we observe a well pronounced internal bore followed by a train of short period internal waves. The mean current opposite to the wave makes the wavelength shorter, and hence the slopes of the internal tide are steeper, which leads to wave breaking and formation of a packet of shorter internal waves. For a uniform westerly current the bore is observed in the entire water column.

West of Camarinal Sill the internal tide propagates in the same direction as the outflowing current. The current increases the wavelength. The internal bore is formed, but only a weak packet of shorter waves appears.

In the third version of the model calculation we have analyzed the internal tide developing in the strait with two opposite currents modeling the real situation. The eastward flow with mean velocities of 50 cm/s occupies the upper 250-300 m layer and the lower current with a vertically average velocity of 25 cm/s occupies the rest of the water column. These two opposite flows yield a strong shear at 200 m depth. The two oppositely directed currents in the stream were introduced in the model by specifying two different vertical distributions of density in the eastern and western parts. In this version of calculations the computational area was increased in the eastern and western directions. In the beginning of the calculations the water was set to flow free under the influence of different density distributions in the eastern and western parts. After the adjustment and formation of a two-layer flow in the central part of the computational area we superimpose the same tidal flow as in the previous versions of calculations. The wavelength of the easterly propagating wave is 90 km. The leading edge of the wave is flatter than the trailing edge, which is very steep. This leads to the formation of internal bore. A train of shorter internal waves follows a sharp depression of density contour lines. The westerly propagating wave is shorter. Its wavelength is 60 km, as the depth west of Camarinal Sill is smaller. The structure of the wave is approximately the same except for the fact that internal bore is less intensive in the western part than in the eastern part of the basin.

The introduction of two opposite currents with a shear intensifies the internal bore in the upper layer at depths of 100-200 m, while in the deeper water it becomes less apparent (Fig. 3c). Intensification of the internal bore and associated short period internal waves in the upper layer in the eastern part obtained in the model calculations confirms the observations at the surface made from satellites, airplanes, and coastal radars that surface manifestations of internal tide are clearly seen in the eastern part of the strait.

## 4 CONCLUSIONS

The main results of this research are the following:

Internal tidal oscillations observed in the Strait are mostly generated over Camarinal Sill.

The observations analyzed depict the generation of internal tides with peak-to-peak amplitudes exceeding 200 m. The waves propagate in both directions from the sill losing energy while

propagating. The major motion of internal tide is associated with the semidiurnal M2 frequency.

## ACKNOWLEDGEMENTS

This research was performed within the framework of the state assignment of Russia (theme no. 0149-2019-0004) and supported in part by the Russian Foundation for Basic Research) (project no. 17-08-00085).

## REFERENCES

- Barber, N.F., 1963. The directional resolving power of an array of wave detectors. In: *Ocean wave spectra*, N.Y., Engelwood Cliffs, Prentice Hall, pp. 137-150.
- Bryden, H.L., Candela, J., and Kinder, T.H., 1994, Exchange through the Strait of Gibraltar, *Prog. Oceanogr.*, **33**, pp. 201-248.
- Morozov, E.G., Trulsen K., Velarde M.G., and Vlasenko V.I., 2002, Internal tides in the Strait of Gibraltar, *J. Phys. Oceanogr.*, **32**, pp. 3193-3206.
- Morozov E.G., Parrilla-Barrera G., Velarde M.G., Scherbinin A.D., 2003, The Straits of Gibraltar and Kara Gates: A Comparison of Internal Tides, *Oceanologica Acta*, Vol. 26 (3), pp. 231-241.
- Vlasenko V.I., 1992, Nonlinear model for the generation of baroclinic tides over extensive inhomogeneities of bottom topography. *Phys. Oceanogr. (Morskoy gidrofizicheskiy zhurnal)*. Vol. 3: pp. 417-424